AD-A138 729 A NEW SATELLITE INSTRUMENT FOR YAW AND PITCH MEASUREMENTS(U) AIR FORCE GEOPHYSICS LAB HANSCOM AFB MA J P MCISAAC 13 SEP 82 AFGL-TR-82-0265 1/1

UNCLASSIFIED F/G 22/3 NL

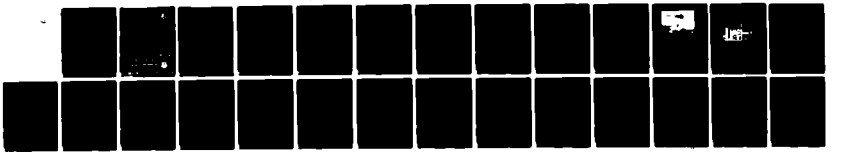

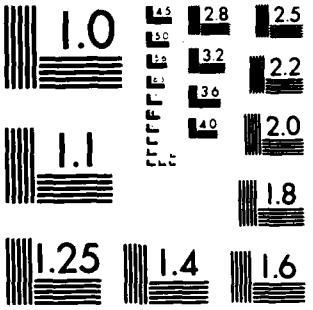

MICROCOPY RESOLUTION TEST CHART
NATIONAL BUREAU OF STANDARDS-1963-A

AFGL-TR-83-0265
INSTRUMENTATION PAPERS, NO. 312

A New Satellite Instrument for Yaw and Pitch Measurements

J.P. McISAAC

13 September 1982

AERONOMY DIVISION PROJECT 6690
AIR FORCE GEOPHYSICS LABORATORY
HANSCOM AFB, MASSACHUSETTS 01731

AIR FORCE SYSTEMS COMMAND, USAF

This report has been reviewed by the ESD Public Affairs Office (PA) and is releasable to the National Technical Information Service (NTIS).

This technical report has been reviewed and is approved for publication.

Alva T Stair Jr.

DR. ALVA T. STAIR, Jr
Chief Scientist

Qualified requestors may obtain additional copies from the Defense Technical Information Center. All others should apply to the National Technical Information Service.

Unclassified

SECURITY CLASSIFICATION OF THIS PAGE (When Data Entered)

REPORT DOCUMENTATION PAGE		READ INSTRUCTIONS BEFORE COMPLETING FORM
1. REPORT NUMBER AFGL-TR-82-0265	2. GOVT ACCESSION NO. AD-A138729	3. RECIPIENT'S CATALOG NUMBER
4. TITLE (and Subtitle) A NEW SATELLITE INSTRUMENT FOR YAW AND PITCH MEASUREMENTS		5. TYPE OF REPORT & PERIOD COVERED Scientific Interim 6. PERFORMING ORG. REPORT NUMBER IP, No. 312
7. AUTHOR(s) J. P. McIsaac		8. CONTRACT OR GRANT NUMBER(s)
9. PERFORMING ORGANIZATION NAME AND ADDRESS Air Force Geophysics Laboratory (LKB) Hanscom AFB Massachusetts 01731		10. PROGRAM ELEMENT, PROJECT, TASK AREA & WORK UNIT NUMBERS 62101F 66900707
11. CONTROLLING OFFICE NAME AND ADDRESS Air Force Geophysics Laboratory (LKB) Hanscom AFB Massachusetts 01731		12. REPORT DATE 13 September 1982 13. NUMBER OF PAGES 26
14. MONITORING AGENCY NAME & ADDRESS(if different from Controlling Office)		15. SECURITY CLASS. (of this report) Unclassified 15a. DECLASSIFICATION DOWNGRADING SCHEDULE
16. DISTRIBUTION STATEMENT (of this Report) Approved for public release; distribution unlimited.		
17. DISTRIBUTION STATEMENT (of the abstract entered in Block 20, if different from Report)		
18. SUPPLEMENTARY NOTES		
19. KEY WORDS (Continue on reverse side if necessary and identify by block number) Spacecraft attitude Yaw Pitch Aspect determination Autonomous detection Satellite sensors Pointing angle indicator Velocity vector		
20. ABSTRACT (Continue on reverse side if necessary and identify by block number) A new device for measuring spacecraft attitude was flown on the Air Force S3-4 satellite. This report describes instrumentation, measurement technique, and operating results. Instrument attack angles were measured during night and day periods of most orbits. Attitude history plots and tables are given for the experiment from April to August 1978.		

DD FORM 1 JAN 73 1473 EDITION OF 1 NOV 65 IS OBSOLETE

Unclassified

SECURITY CLASSIFICATION OF THIS PAGE (When Data Entered)

Preface

The author thanks D. Sipler and R. Huffman for their helpful suggestions and review of the paper, Dennis Delorey of Boston College's Space Data Analysis Laboratory for plotting routines, and Stephanie Furlow for manuscript preparation. K. Wright and H. Donald of A.F. Space Division and R. Knauss of Aerospace Corporation are owed a special thanks for their support throughout the program.

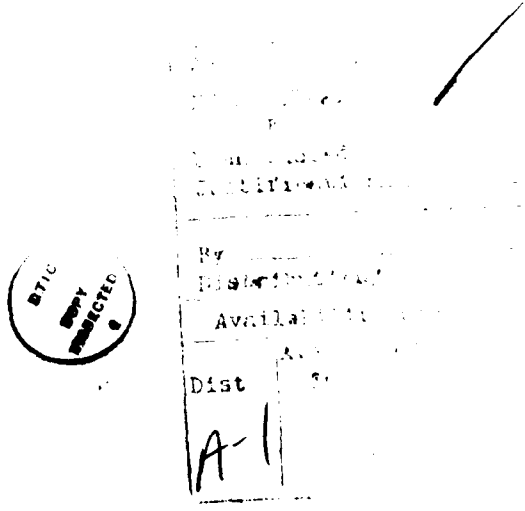

Contents

Illustrations

Tables

A New Satellite Instrument for Yaw and Pitch Measurements

1. INTRODUCTION

Two neutral density measurements systems were flown on the S3-4 satellite and successfully operated during 1978. Observations were obtained over a six-month operating period. Both measurement systems were programmed to operate in either of two modes: a primary mode during which atmospheric neutral density would be measured and a secondary mode during which the measurement system acted as an attitude sensor. This report describes the operation and results obtained from the measurement systems that function as attitude sensors during secondary-mode operation. Proof of principle and practicality for operations of this type has been demonstrated and verified by the large number of accurate angular measurements performed throughout the six-month experiment. Some description of primary-mode operation has been included here insofar as it relates to the understanding of secondary-mode operation. However, the primary purpose of this report is to describe the performance of the flight instrumentation as an attitude sensor as well as to indicate some potential options and applications available for future development.

(Received for publication 10 September 1982)

2. ORBIT PARAMETERS

The experiment was placed into orbit onboard a DOD designated S3-4 satellite in 1978. The orbit was polar inclined with a perigee of 165 km and an apogee of 265 km. The satellite was three-axis stabilized during experiment operation. Normal experiment operations began in April 1978 and continued routinely every day over the six-month period of experiment operation.

The normal data acquisition cycle was a 20-day period; 3 consecutive days of 20 minute segment passes centered around perigee followed by 17 consecutive days of either full-orbit passes (~90 min) or half-orbit passes (~45 min) depending upon which of two telemetry sampling rates were selected. Overall, from four to six full orbit passes would be obtained on a daily basis and a larger number of partial passes would be acquired if the faster telemetry rate was employed.

The neutral density experiment operated throughout the six-month period without mishap or malfunction during both primary and secondary mode operations, although some anomalies were seen. One such anomaly occurred at a point approximately two-thirds into the mission life and will be discussed later in this report.

3. FLIGHT INSTRUMENTATION

3.1 Function

The primary function of the payload experiment was to sample and measure the density of the atmospheric gas at orbit altitudes. This was accomplished through the use of an ionization gauge that opened to the ambient atmosphere once orbit was obtained; whereupon, atmospheric gases would flow into the gauge at satellite velocities. Incoming gas produces a buildup of internal gauge density far in excess of the external atmospheric gas density. A portion of the internal gas density is ionized, collected, and measured. This measurement, in turn, can be related to and is a function of the ambient atmospheric gas density. The relationship between the gauge internal density and the ambient atmosphere under the conditions of satellite flight has been described in detail in previous reports.[1,2]

---

1. McIsaac, J. P., McInerney, R. E., and Delorey, D. (1978) Satellite Ionization Gauge Measurements of Atmospheric Density, AFGL-TR-78-0201, AD A061613.

2. McIsaac, J. P., Champion, K. S. W., McInerney, R. E., and Delorey, D. (1976) Ionization Gauge Measurements of Atmospheric Density From a Low Altitude Satellite, AFGL-TR-76-0113, AD A032373.

This operating function is defined as the primary operating mode of the payload experiment. One other operating mode, the subject of this report, is referred to as the secondary mode.

The secondary operating mode involves the interruption of the atmospheric gas flow (airstream) into the ionization gauge. During this time period when gas flow interruption occurs the experiment operates as an attitude sensor. To cause this flow or airstream interruption a blocking or baffling operation has to be initiated. Additional hardware was added to the ionization gauge sensor in order to accomplish this blocking/baffling action. This hardware is referred to as the baffle assembly. The ionization gauge sensor and its electronics are combined with the baffle assembly to make up the total operation apparatus of the attitude sensor.

3.2 Description

The neutral density experiment, also the attitude sensing experiment, consisted of two units referred to as the cold cathode gauge (CCG) unit and the particle flux accumulator (PFA) unit. With a few exceptions the CCG unit is identical to the PFA unit. The exceptions include baffle arm locations, gauge entrance conductances, and baffle-arm deployment rate. Both the CCG and PFA units contained magnetron type ionization gauges equipped with baffle assembly devices that were employed when the units operated as attitude sensors. Magnetron gauges do not require hot filaments as do the more conventional type ionization gauges but, rather, utilize crossed magnetic and electric fields in their operation. Initial gauge operation begins when 1800 V are applied to the anode electrode, whereupon an electric discharge is established. Positive ions extracted from this discharge produce a current output that varies proportionally to the internal gas density of the gauge.

Figure 1 is a photograph of the PFA flight system before delivery for spacecraft installation. Table 1 provides some instrument specifications in addition to listing some of the preflight tests that were conducted on the units. The right-hand box in Figure 1 houses most of the electronic circuitry required in the experiment operation. Included in this unit are low voltage supplies, signal amplifiers, and monitoring, calibrating, conditioning, and timing circuitry. The left-hand unit (with its cover removed) is the sensor unit; containing the ionization gauge, magnet, high voltage power supply, baffle, baffle motor, and a gauge uncapping mechnism. The uncapping mechanism is required as the ionization gauge is evacuated and hard sealed (once broken cannot be resealed) before installation on the satellite and subsequently opened only after orbit is obtained. Using this procedure the shelf life of the gauge, its ability to retain an internal vacuum, has

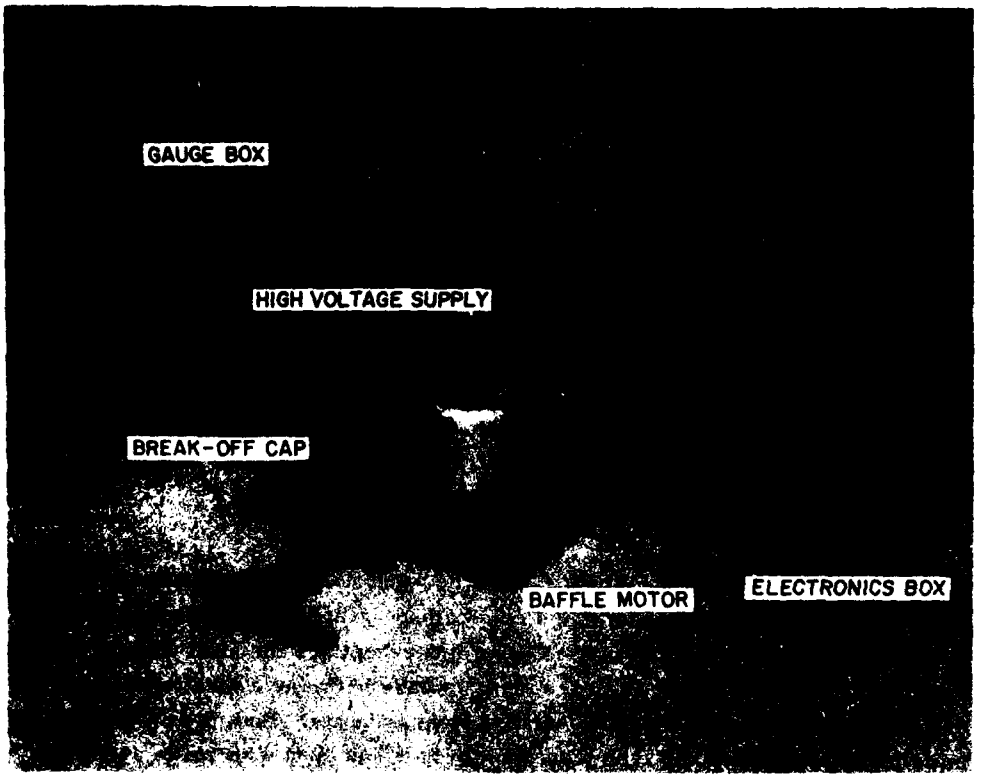

Figure 1. Flight Instrument for Attitude Measurements

exceeded a year. An alternative to hard sealing the gauge would be to attach the unit to a vacuum pump system each time it is to be operated, however, this is a cumbersome and time costly procedure.

Figure 2 is a side view of the PFA sensor and provides a better perspective of the relative size and location of the various sensor components. The breakoff or uncapping mechanism is shown with the gauge uncapping lever in its activated position. This is the locked-in upright position of the lever arm after in-orbit activation. The baffle is seen in a deployed position and the width of the baffle can be compared to the dimension of the gauge sensing tubulation, which is the capped tube seen protruding out from break-off mechanism. The baffle, as explained later, serves to block the in-orbit airstream flow into the gauge sensor.

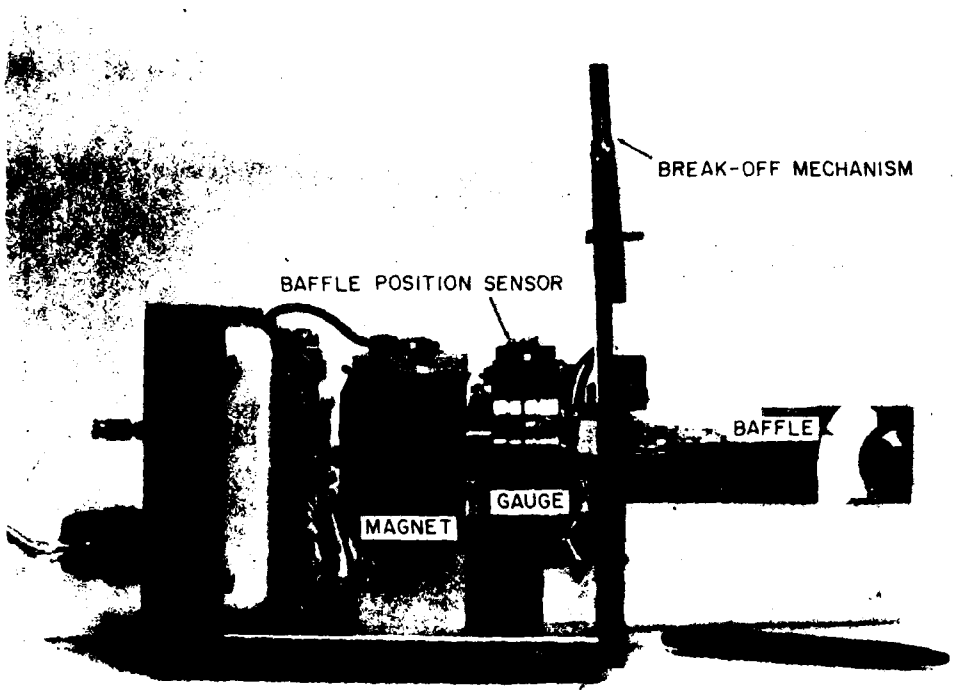

Figure 2. Sensor Unit

Table 1. Flight Instrument Specifications

Size:	sensor unit	-	5" × 5" × 6.5"
	electronic unit	-	8" × 4.5" × 4.5"
Weight:	sensor unit	-	9 lb
	electronic unit	-	3.75 lb
Operating Power:			5.6 W at 28 Vdc
View Direction:			nominal 45° to the velocity vector
Field of View:			30° (half angle cone)
Baffle Arm Length (max):			PFA - 3.69 in. CCG - 3.95 in.
Baffle Arm Width:			PFA - 1.45 in. CCG - 1.45 in.
Baffle Deployment Period: (extension and retraction)			PFA - 56 sec CCG - 63 sec
Environmental Testing:			EMI - MIL STD 826
			Variation - Random at 12g rms 20 to 2000 hz
			Thermal Vacuum
			Duration - 48 h
			Pressure - less than 10^{-5} torr
			Temperature - [illegible]

4. BAFFLE MODE OPERATION

In order to fully understand how the baffle deployment [illegible] aspect angles, the directional relationship between gas particle flow and the velocity vector should be known. The flow of particles (molecules and/or atoms) at satellite velocity into the gauge sampling orifice generates a signal that is proportional to the airstream velocity. Airstream direction is always in the same direction as the velocity vector only opposite in sense (that is, 180° out-of-phase). Hence, when the airstream direction is determined, the velocity vector direction is known.

As previously stated, the baffle mode of operation provides a system response that can now be interpreted to determine instrument aspect angle. In this particular application the aspect angle measured is the angle between the velocity vector and the principal axis of the gauge sensor. If, however, the principal axis of our instrument were properly aligned on the vehicle's yaw or pitch axis, which was not

the case for this flight, then the aspect angle measured by the instrument would be the yaw or pitch angle, respectively. Our instrument was mounted on an intermediary axis that was located at an angle to both the yaw and pitch axes of the spacecraft. Figure 3 shows schematically various positions of the baffle arm in relationship to the airstream and the gauge sampling inlet. The following explanation describes what occurs as the baffle arm is activated and deployed to extend and intercept the airstream. The small vertical arrows seen in Figure 3(c) at the base of the baffle arm indicate the direction of baffle arm motion.

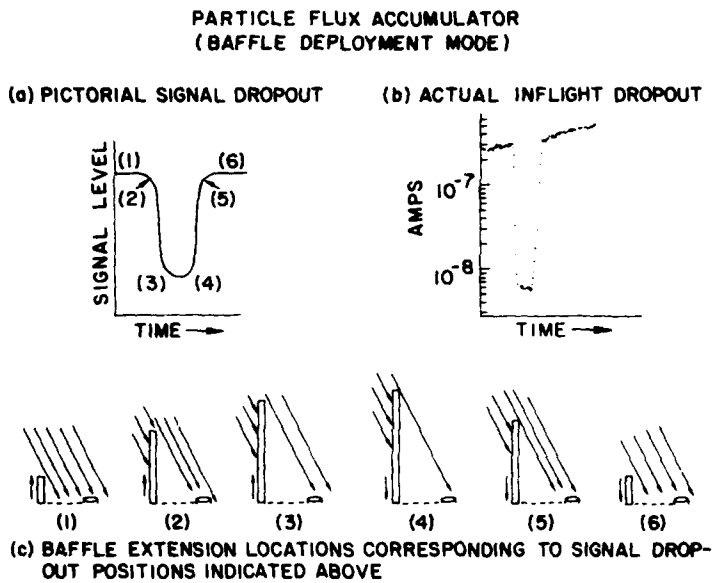

Figure 3. Schematic Drawing of Baffle Deployment Signal

Referring to location (1) of Figure 3(c), the baffle arm is seen extending upwards but not yet intercepting any of the airstream lines impacting the gauge inlet area; correspondingly, the system output signal remains unaffected by the extension. The sensor output signal at this time is seen as point (1) in Figure 3(a). In location (2) (Figure 3(c)) the baffle arm extends to a position where it begins to intercept the airstream lines (gas flow) which, if left unimpeded by the baffle arm, would, in their normal course, enter the sampling orifice. The effect upon

the system output signal of this initial occultation of the gauge inlet area can be seen in Figure 3(a) where at point (2) we see the signal output start to fall off. The signal output continues to decrease as the baffle arm in its upward travel intercepts more and more of the airstream lines until the position shown in location (3) Figure 3 is reached. In this position all the airstream lines that would have reached the gauge inlet area have been occulted (baffled). The inlet area remains fully occulted while the baffle arm travels its full extension whereupon at maximum extension the arm trips an optical limit switch that initiates a baffle return command. The baffle arm, now retracting, continues to occult the inlet area until in its downward travel the location (4) shown in Figure 3(c) is reached, whereupon further travel begins to expose or uncover the gauge inlet area. This uncovering action continues as the arm travels further downward until the inlet area is fully exposed [location (5)] to the gas flow and ambient conditions are again restored [location (6)]. Again, signal output response can be seen in Figure 3(a); points (3) and (4) are the transition points corresponding to location (3) and (4) in Figure 3(c) where the points represent the initial and final positions of full occultation respectively, point (5) [Figure 3(a)] shows the transition point to a fully exposed inlet and point (6) shows where fully-restored ambient conditions prevail. Baffle arm retraction ends when the arm trips an optical limit switch at its stowed position. Figure 3(b) is an actual inflight response of the system during a typical baffle deployment operation.

One further characteristic of system response should be noted. If the aspect angle remains constant over the period of a baffle arm excursion then the signal output curve should be symmetrical with regard to baffle arm extension lengths. That is, the baffle arm extension length at locations (2) and (5), Figure 3(c), are equal. Later it will be discussed how this observation provides additional corroboration of the results obtained from the angular measurement technique.

4.1 Baffle Angular Determination

The sensor output signal together with the baffle arm extension monitor signal are combined in an illustrated plot, Figure 4, in order to show more clearly how the technique works to measure the instrument's aspect angle. Referring to Figure 4(b), the triangular shaped, dashed output trace represents the baffle arm extension length as a function of time, whereas the solid trace is the gauge output showing a signal dropout (as has been described previously). At times t_1 and t_2, the baffle arm position is equal to y_1 and y_2, respectively, where y_1 is the position at which the arm just begins to occult the gauge inlet area in its upward travel and y_2 is that arm position in its downward travel where the gauge inlet area becomes fully exposed from its previous occulted phase. At either time the angle β as shown in Figure 4(a) and the attack angle are as follows:

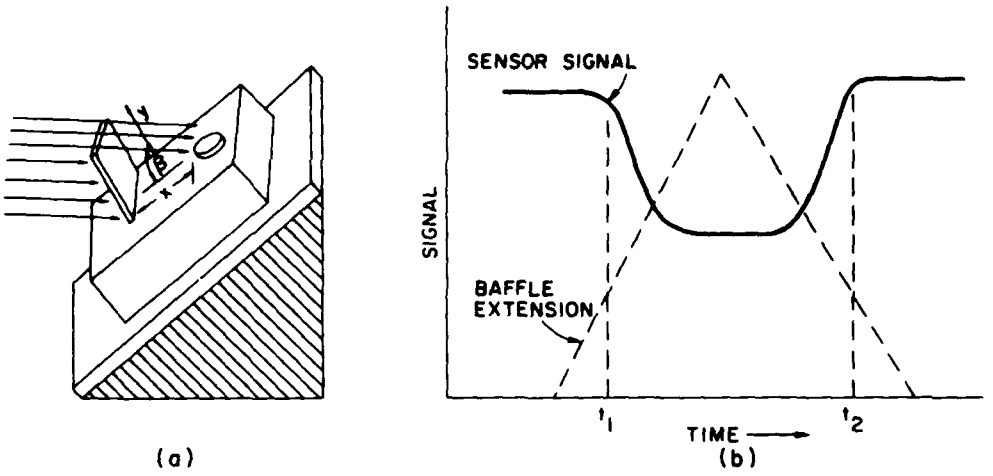

Figure 4. Schematic View of Baffle Obscuration

$$\beta = \tan^{-1} y/x \quad (1)$$

$$\text{attack angle} = 90^{\circ} - \beta \quad (2)$$

where the distance y is the baffle arm length at the times and the distance x is the lateral distance from the baffle to the inside edge of the gauge sampling orifice. The attack angle is defined as the angle between the velocity vector and the instrument sampling axis. The sensor's sampling axis and the baffle arm were made parallel to each other in the design of the instrument hence the angle β measured earlier is the complement to the attack angle of the instrument. This is easily seen in Figure 5 where the relevant dimensions and angles are defined at the two times previously discussed. It should be further noted that during each of the two times, t_1 and t_2, of the baffle deployment cycle an angular determination is performed. If the attack angle remains constant during the deployment cycle then y_1 will equal y_2. However, if the angle should change during the time interval from t_1 to t_2 then that change will be detected, since y_2 will no longer equal y_1 but rather will vary in accordance to how the attack angle varied. The baffle length, y, will become shorter if the attack angle increased and longer if the attack angle decreased. Figure 5 depicts a situation where the attack angle has decreased during the time interval from t_1 to t_2, where y_2 is larger than y_1.

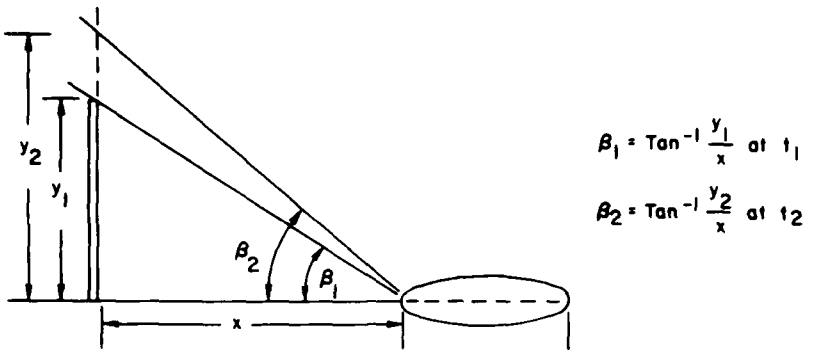

Figure 5. Schematic Drawing of Relevant Angles and Dimensions

5. RESULTS

Gauge vacuum caps that sealed the sensor's inlet tubulation were explosively ejected during the initial satellite orbits. When success was confirmed, the PFA unit was powered on and secondary-mode operational checkouts were performed. Nine consecutive baffle deployment cycles were ground commanded and executed over a 15-min interval. Quick-look data were obtained and examined in order to determine if the appropriate response was elicited before initiating the CCG baffle deployment checkout. Following the successful PFA baffle checkout, the same procedure was performed for the CCG unit. Figure 6 is a photograph of a microfiche record showing the CCG unit's response to the nine baffle deployment commands given during that inflight checkout. The attitude angle as measured by the CCG unit is shown above each deployment signal dropout. Note that the attitude angle varies from 49° to 45° as the satellite descends to lower altitudes. This variation of spacecraft attitude occurs regularly during the experiment as will later be seen from the flight history graphs.

Routine experiment operations began in April 1978. For both the PFA and CCG units, routine secondary-mode operation consisted of two deployments one each on the dayside and nightside of the orbit, for every data acquisition revolution except during the three day periods when 20-min perigee were being obtained. During the periods of perigee pass acquisitions no secondary telemetry mode operations were commanded. The command routine usually exercised on each revolution involved first commanding the PFA baffle deployment on during the nightside of the orbit followed within approximately one minute by a CCG baffle deployment command. Around one hour later the same routine PFA baffle

S3-4 BAFFLE DEPLOYMENT MODE

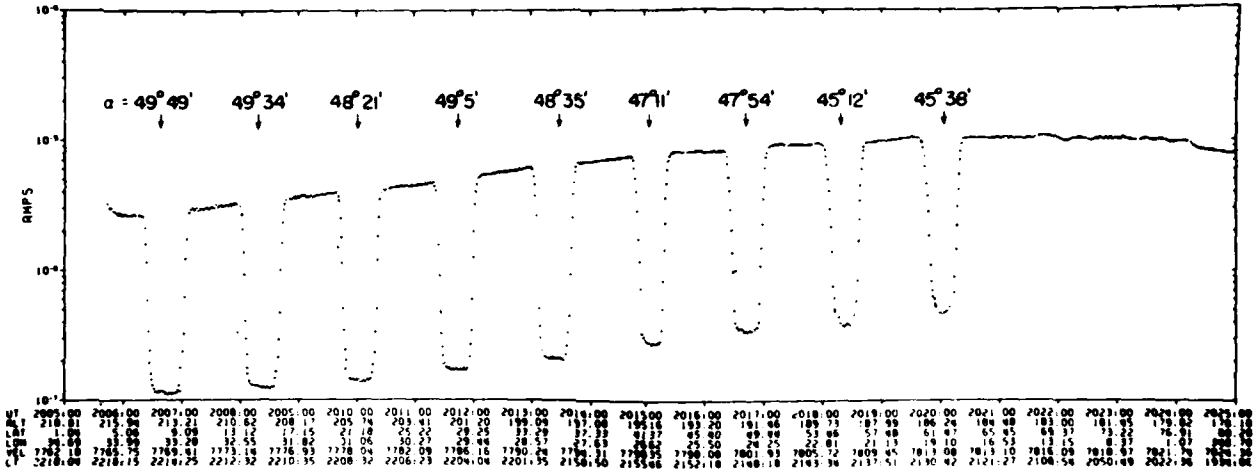

Figure 6. Checkout Revolution for CCG Unit

deployed followed a minute later by the CCG baffle command would be repeated only this time with the satellite traversing the sunlit portion of the orbit.

Flight history plots of attitude angle measurements performed over the six-month experiment operating period are shown in Figures 7 and 8. The data have been compressed into a more manageable form by averaging the measured values over intervals of 33 revolutions and plotting the average value for the interval as a single point. Table A1, in Appendix A, shows the average value and the number of values averaged in each of the 33 revolution intervals. Where the first revolution is the initial revolution marking the beginning of routine experiment operations. Many more measurements remain to be examined and assessed now that observations for the entire experiment have been received.

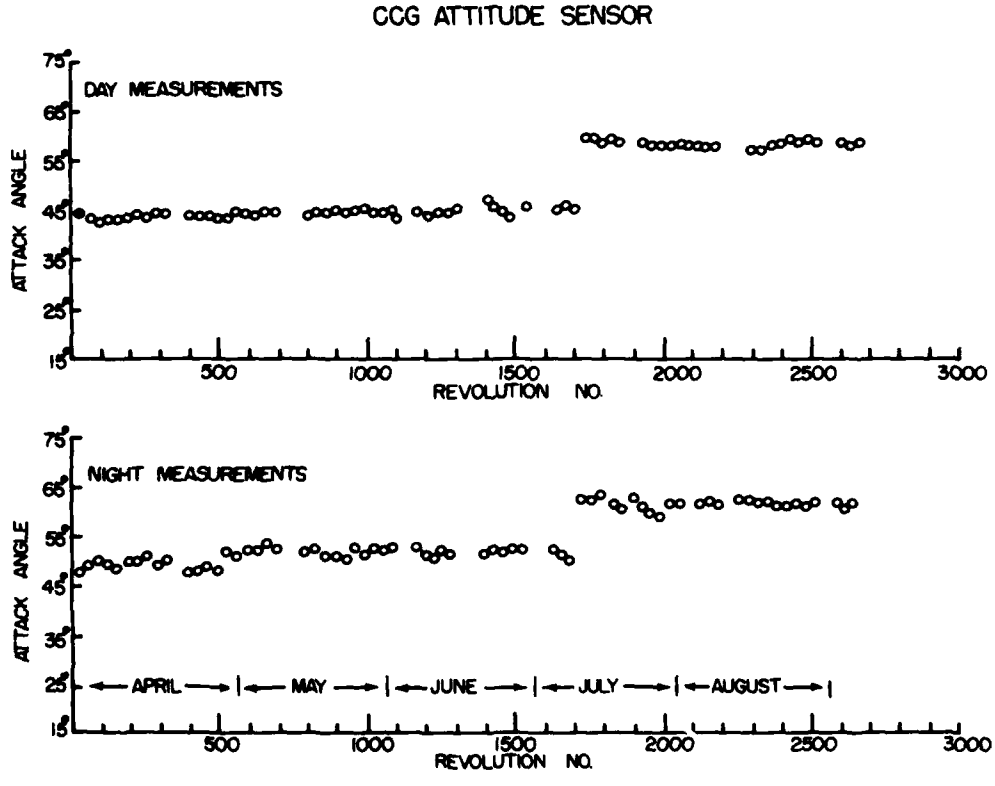

Figure 7. Experiment Attitude History

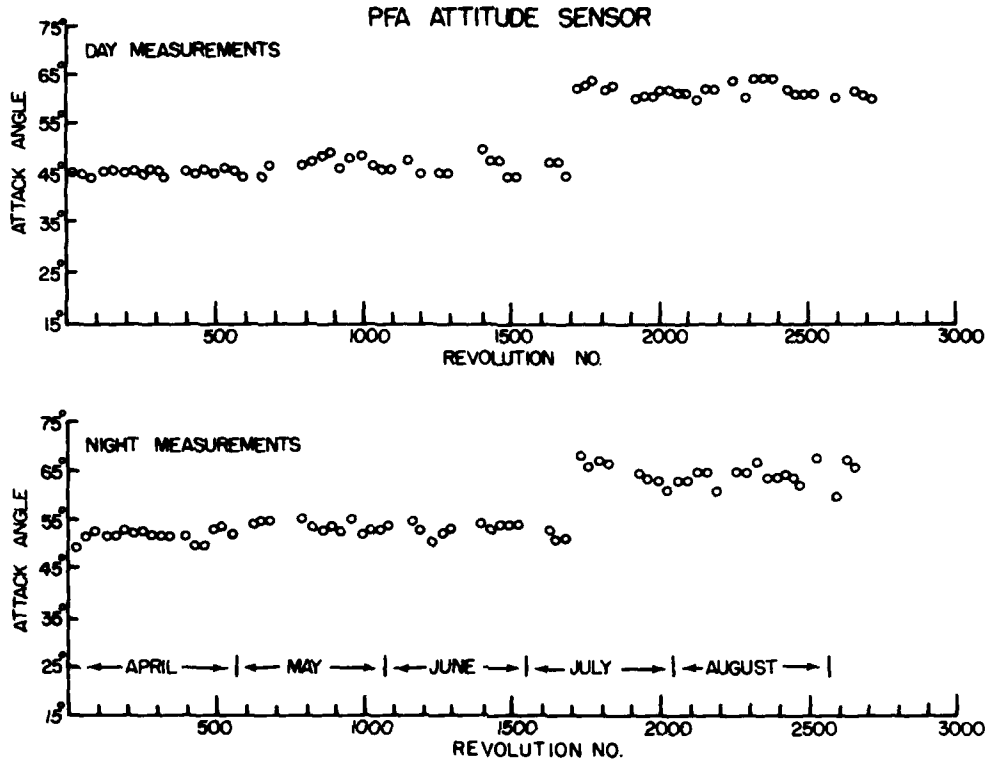

Figure 8. Experiment Attitude History

6. DISCUSSION

Our flight history measurements as shown in Figures 7 and 8 indicate that the spacecraft attitude control was maintained throughout the six-month period of operation although not fully in the manner specified in preflight planning sessions. Preflight plans called for a fixed pointing orientation of 45° from the spacecraft velocity vector for both the PFA and CCG units. The instrument mounting specifications given by the spacecraft contractor for instrument pointing accuracies were as follows:

Pitch - within 1.77°
Roll - within 2.02°
Yaw - within 2.25°.

Our measurements show that the 45^{o} attack angle specification for both the PFA and CCG was maintained in flight only during the low-altitude portion of the orbit and then only until mid-July. The small discrepancy between the overall measurements between the PFA and CCG is attributed to inaccuracies in the mounting of the units within the spacecraft; as the differences are within the given specifications. The greater scatter seen in the PFA measurements is believed due to the slower conductance of the PFA unit relative to the CCG unit.

A further verification of the results seen in the flight history plots can be obtained from the baffle deployments performed during the experiment checkout phase; see Figure 6. In Figure 6 one observes the experiment attitude slowly varying from the high-altitude aspect angle of 49^{o} to a lower altitude aspect angle of 45^{o}. This, of course, is the same behavior observed in the history plots; namely, larger attack angles being seen during high altitude deployments than are seen during low altitude deployments. This same behavior is also observed after mid-July only now a 15^{o} shift to larger attack angles has occurred. The shift in attack angle of approximately 15^{o} after mid-July is maintained over the orbit for the remainder of the mission. Also confirming the 15^{o} increase in attack angle measurements is the observance of an increase in the width of the baffle deployment dropout signal which should occur if the attack angle increases. By width of the dropout signal is meant the distance from point (2) to point (5) as seen in Figure 3(a). A significant increase in dropout signal width did occur in all deployment cycles after mid-July, further confirming the truth of the measurements.

Insofar as the accuracy of the attitude measurements are concerned one can state that they are within the range of uncertainties given above for mounting accuracy. An independent measurement set of data was not made available to the experimenters hence our measurement accuracy must be indirectly evaluated. In assessing the accuracy of the baffle measurement technique from ground calibration routines, namely that of dimensionally scaling all the relevant distances to controlled tolerances our estimate of accuracy for the measurement is $\pm 0.5^{o}$. It should be noted that a 1 percent error in the baffle dimensions results in only a 0.25^{o} uncertainty in the angular determination. A 1 percent dimensional tolerance is not a difficult accuracy to obtain.

7. AIR FORCE APPLICATIONS

Among the potential uses to the Air Force are the following:

(a) Technique fulfills a need for a simple, inexpensive system for use in the measurement of pitch and yaw attack angles,

(b) Allows for the cost effective and practical instrumentation of large-scale space structures with a large number of detectors for attitude sensing in a distributive attitude detection system,

(c) Possesses the ability to perform sensing measurements at vehicle's or station's extremities, positions avoided by inertial systems due to elastic deformation (bending). Applicable to large-scale flexible space structures,

(d) Provides a low-cost supplement to current satellite attitude transducers and increases system reliability through the use of a different technology,

(e) Suitable for autonomous spacecraft operation, particularly, if that operation is independent, that is, without reliance upon sources external to vehicle as for example a stellar or sun reference,

(f) Can be operated at any time and position in orbit,

(g) Use as a determinant of attitude system failure. In many cases failure detection takes a higher priority than system performance evaluation (that is, analytical attitude determination tool),

(h) Possible to develop self-contained, transportable unit for use in space maintenance functions such as in-orbit installations of replacement unit in servicing of recoverable satellites,

(i) Use as a pointing indicator referenced to the velocity vector, by installing gimbal mount,

(j) Useful as a real-time attitude reference for periodic in-orbit update of gyro systems,

(k) Amenable to radiation hardening and to operation in severe and "cluttered" space environments,

(l) Adaptable for application as a manual indicator of attack angles experienced during an astronaut's extravehicular activities.

The accomplishment of many of these applications appears much more attainable when one realizes that the experiment baffle design was based on a premise of minimum interference to the principal experimental operating mode that was ambient density measurements and not attitude sensing. As a result of that premise only a very simple and economical attitude sensing design was developed. With this simple design, the main objective of the secondary-mode operation was to provide proof of principle for the attitude sensing technique.

That goal having been realized with the success of this experiment, current plans call for the upgrading of the present design of the attitude sensors. For instance, a minor modification involving adding a second baffle and reconfiguring the location of the baffles would enlarge the attitude sensor's field of view to 180° about the velocity vector.

If additional funding is obtained then the experience and knowledge accrued from the successful S3-4 experiment could be applied towards the development of improved instrument designs using the baffle sensing technology.

8. CONCLUSIONS

From the successful flight test results, a novel and versatile technique for yaw and pitch attitude angle measurements has been proven. Yaw angle measurements, which are the most difficult to realize,[3] present no inherent obstacles and can be performed in the same manner as pitch angle measurements. As earlier stated, the instrument's principal axis was not positioned onboard the spacecraft's pitch or yaw axis hence our measurements are not an actual demonstration of pitch and yaw angle measurements. However, the results obtained from our attitude measurements do demonstrate that with proper instrument installation the attitude angles measured can be made into pitch and yaw angle measurements. The accuracy of the attack angle measurements was estimated to be $\pm 0.5^{\circ}$. However, design parameters could be optimized to enhance the attitude sensing capabilities of the present sensors to increase the $\pm 0.5^{\circ}$ accuracy to $\pm 0.1^{\circ}$. Finally, if future funding becomes available, further development of the technique could be accomplished thereby expanding the Air Force's inventory of spacecraft sensors available for applications in future DOD space activities.

---

3. Floyd, F.W., Much, C.H., Smith, N.P., Vernaw, J.R., and Woods, J.P. (1980) Flight performance of the LES-8/9 three-axis attitude control system, Proceedings AIAA 8th Communication Satellite Systems Conference:159-169.

Appendix A

Table of Averages

Table A1. Average Values and Number of Data Points

Orbit Interval	N^+	α^+_{PFA}	N^*	α^*_{PFA}	N^+	α^+_{CCG}	N^*	α^*_{CCG}
1-33	5	45.2	8	49.1	8	44.4	8	47.7
33-66	10	44.7	24	51.9	10	43.2	11	49.3
66-100	18	43.9	20	52.7	18	43.6	17	50.6
100-133	13	45.8	22	51.7	11	43.9	19	49.3
133-166	12	46.3	21	52.1	10	43.8	18	48.8
166-200	18	45.3	22	53.0	16	44.0	24	49.8
200-233	17	45.8	20	52.6	13	44.8	20	49.7
233-266	9	44.5	16	52.6	12	43.8	13	50.8
266-300	14	45.6	16	51.6	12	44.9	20	49.2
300-333	10	45.1	12	51.3	8	44.8	10	50.0
333-366	0	-	0	-	0	-	0	-
366-400	4	46.0	8	51.7	2	44.2	2	47.9
400-433	6	44.9	11	49.1	6	43.9	10	45.9
433-466	3	45.6	8	50.3	4	44.8	8	49.0
466-500	2	45.0	6	53.5	2	43.5	8	47.9
500-533	1	46.7	8	54.2	2	43.1	6	52.3
533-566	3	46.0	12	52.4	4	44.1	11	51.3
566-600	2	44.5	0	-	2	43.9	2	51.9
600-633	0	-	4	53.5	2	44.2	4	52.3
633-666	2	44.3	4	54.9	2	45.2	4	52.7
666-700	4	47.5	7	54.8	4	44.6	8	52.2
700-733	0	-	0	-	0	-	-	-
733-766	0	-	0	-	0	-	-	-
766-800	2	46.0	4	55.2	2	44.4	4	52.4
800-833	4	47.6	6	53.9	4	45.5	8	53.0
833-866	2	48.0	4	52.1	2	45.0	2	51.1
866-900	4	49.3	8	53.2	3	46.3	8	49.9
900-933	2	45.4	4	52.1	2	44.8	4	50.5
933-966	2	47.8	4	55.1	2	45.7	2	53.4
966-1000	4	48.1	8	51.7	3	45.0	8	51.1
1000-1033	5	46.7	8	53.2	3	44.8	8	52.6
1033-1066	3	45.7	2	50.2	4	45.2	4	52.0
1066-1100	1	45.7	8	52.9	2	44.1	2	52.9
1100-1133	0	-	0	-	0	-	0	-
1133-1166	7	47.6	6	54.3	3	45.5	6	53.1

Table A1. Average Values and Number of Data Points (Contd)

Orbit Interval	N^+	α^+_{PFA}	N^*	α^*_{PFA}	N^+	α^+_{CCG}	N^*	α^*_{CCG}
1166-1200	4	44.5	2	51.7	1	44.4	4	51.6
1200-1233	4	47.1	8	50.7	2	45.5	8	51.0
1233-1266	6	44.9	7	51.3	4	44.5	8	51.6
1266-1300	2	44.7	6	53.3	4	44.8	8	51.0
1300-1333	0	-	0	-	0	-	0	-
1333-1366	0	-	0	-	0	-	0	-
1366-1400	2	50.2	9	54.0	2	47.9	9	52.2
1400-1433	4	46.9	8	52.6	4	45.9	8	52.6
1433-1466	2	42.4	4	53.5	2	44.0	4	51.9
1466-1500	6	44.0	12	53.9	6	44.1	12	50.9
1500-1533	4	44.7	10	53.8	4	45.9	12	51.8
1533-1566	0	-	0	-	0	-	0	-
1566-1600	0	-	0	-	0	-	0	-
1600-1633	3	47.6	4	52.1	4	45.6	4	51.6
1633-1666	5	47.0	4	50.2	4	46.0	4	50.6
1666-1700	8	44.4	7	50.0	5	46.0	10	49.5
1700-1733	8	62.0	16	67.6	8	60.4	16	63.0
1733-1766	7	62.5	12	65.8	10	60.3	12	62.5
1766-1800	2	63.6	6	67.4	2	59.4	8	63.0
1800-1833	4	61.0	2	54.8	4	58.9	8	62.0
1833-1866	4	61.6	6	65.8	2	58.9	8	62.4
1866-1900	0	-	0	-	0	-	0	-
1900-1933	4	60.9	4	63.7	4	58.8	4	61.3
1933-1966	6	60.9	8	62.3	5	58.8	8	60.2
1966-2000	2	61.7	6	62.0	2	59.2	2	58.7
2000-2033	4	59.9	4	60.4	2	58.7	4	62.3
2033-2066	8	61.8	8	63.0	4	58.1	8	62.3
2066-2100	6	60.6	2	62.5	4	58.7	0	-
2100-2133	4	61.6	4	64.6	4	58.4	4	61.6
2133-2166	4	62.8	12	65.8	2	57.8	12	62.4
2166-2200	6	61.9	8	60.7	4	58.0	8	61.9
2200-2233	0	-	0	-	0	-	0	-
2233-2266	3	64.0	6	65.1	2	59.1	4	62.6
2266-2300	8	60.4	8	63.1	6	59.1	6	62.4
2300-2333	2	64.0	4	67.6	1	57.5	4	62.5

Table A1. Average Values and Number of Data Points (Contd)

Orbit Interval	N^+	α^+_{PFA}	N^*	α^*_{PFA}	N^+	α^+_{CCG}	N^*	α^*_{CCG}
2333-2366	4	63.9	6	63.5	2	58.7	8	62.3
2366-2400	8	63.7	6	64.4	4	59.2	8	61.5
2400-2433	4	61.7	4	63.5	2	60.6	2	61.3
2433-2466	8	62.7	8	64.3	4	59.4	8	62.3
2466-2500	6	61.2	7	60.5	4	60.0	8	61.6
2500-2533	4	61.6	4	66.6	4	58.8	8	62.3
2533-2566	0	-	0	-	0	-	0	-
2566-2600	4	62.1	5	59.6	4	59.6	8	60.8
2600-2633	6	62.0	4	67.4	6	58.7	8	61.6
2633-2666	6	61.3	6	64.8	6	58.8	8	62.6
2666-2700	2	61.7	4	66.1	2	59.4	4	66.1

$^+$day measurements
*night measurements